

Technical Paper

Int'l J. of Aeronautical & Space Sci. 13(4), 507–514 (2012)
DOI:10.5139/IJASS.2012.13.4.507

Internal Flow Dynamics and Regression Rate in Hybrid Rocket Combustion

Changjin Lee*

Dept. of Aero, Konkuk University, Seoul, Korea

Abstract

The present study is the analyses of what has been attempted and what was understood in terms of improving the regression rate and enlarging the basic understanding of internal flow dynamics. The first part is mainly intended to assess the role of helical grain configuration in the regression rate inside the hybrid rocket motor. To improve the regression rate, a combination of swirl (which is an active method) and helical grain (which is a passive method) was adopted. The second part is devoted to the internal flow dynamics of hybrid rocket combustion. A large eddy simulation was also performed with an objective of understanding the origin of isolated surface roughness patterns seen in several recent experiments. Several turbulent statistics and correlations indicate that the wall injection drastically changes the characteristics of the near-wall turbulence. Contours of instantaneous streamwise velocity in the plane close to the wall clearly show that the structural feature has been significantly altered by the application of wall injection, which is reminiscent of the isolated roughness patterns found in several experiments.

Key words: regression rate, hybrid rocket combustion, internal flow interaction, vortex shedding

1. Introduction

The interest for hybrid rockets has been revitalized recently not only by its excellent safety features in combustion but also by its low development cost and good thrust controllability [1-2] even though there are many disadvantages in fuel efficiency and the low regression rate. The addition of AP and Al will substantially increase the heat release and lead to improve the regression rate. The second approach resorts to swirl flow in the oxidizer stream injected into the fuel port. The swirl flow can also increase the residence time (or contact time) of the oxidizer stream with the fuel surface. Yuasa et al. [3] designed several swirl injectors and tested the effect of swirl strength on the regression rate. Their results revealed that the average regression rate increases up to 200% as the swirl number increases. However, the enhancement of regression rate is severely localized near the inlet of the fuel port.

A useful approach to increase the burning area was proposed by using helical grooves inside the fuel grain [4].

Even though the use of helical configuration was proved to be very beneficial in increasing the regression rate, the role of the helical grain was not clearly understood in the combustion process. It was conjectured that helical grooves with a low pitch number may produce strong turbulences in the flow since grooves likely act as a turbulent generator. However, for grooves with a higher pitch number, the turbulence structures in the near-wall region exhibited very different behavior from those observed in the grooves with a low pitch number. It is natural to seek an optimal condition of helical grain to maximize the regression rate.

Also, experimental tests by Lee et al. [5] recently reported that small scaled dimples were observed on the surface of hybrid fuel with polymethyl methacrylate/gaseous oxygen (PMMA/GOX) during the combustion. The formation of dimples is presumably attributed to the interaction of the oxidizer stream with the evaporative fuel flux. The formation of dimples is the manifestation of small scale combustion instability in the hybrid rocket combustion. Evans et al. [6] also reported similar dimples on the fuel surface of

the combustion with N₂O/HTPB combination. The size of dimples is much bigger than that found in the previous test. Combustion visualization found very interesting physical features on the fuel surface during the combustion. Visualizations demonstrated that small scale dark spots pop up randomly on the fuel surface covered with dark unburned soot. LES calculation suggests the modified turbulent structures dominantly appear in the after half of the fuel surface. After ignition, flow structures in PMMA show a typical feature of turbulent flow with the coherent axial structure.

In this study, the effectiveness of helical grooves on the increase in regression rate will be reviewed in several test configurations; with and without swirl. Also, the calculation results with the LES (large eddy simulation) study will be summarized to figure out the characteristics of hydrodynamic instability of internal flows in the combustion field. Extensive numerical investigations of non-reacting flows will be presented and reviewed. It is expected that the calculation results will reveal the unique features of hybrid rocket internal flow.

2. Experimental Setup

Figure 1 shows the schematic of the experimental setup

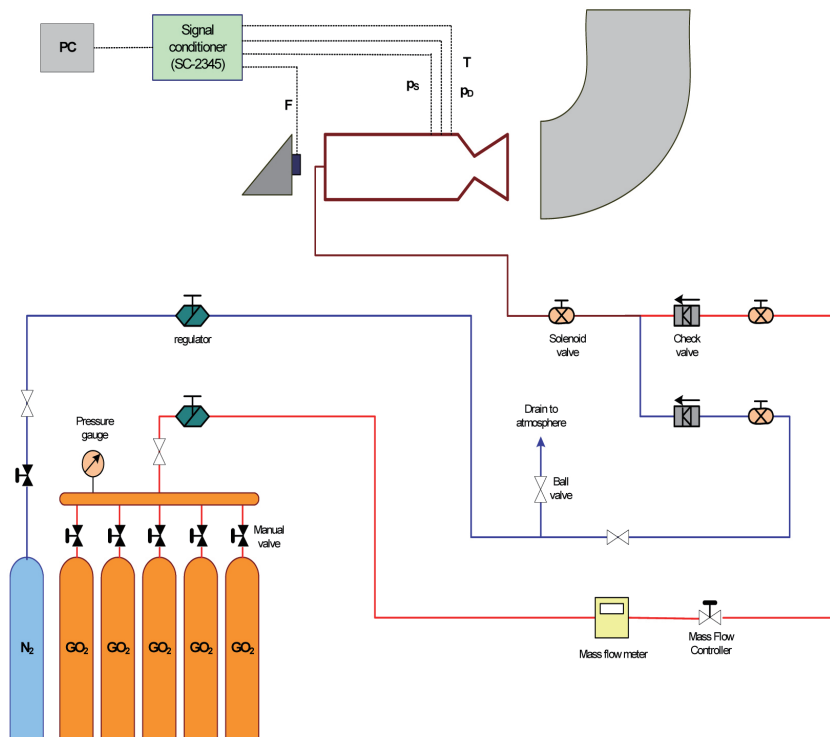


Fig. 1. Schematic of experimental setup

and configuration. PMMA (Poly Methyl Methacrylate) was used as a fuel used in the test and the gaseous oxygen as an oxidizer. Solenoid and check valves control the oxidizer feeding time and nitrogen gas flow rate to purge after the combustion by PLC (Programmable Logic Controller) control. The test utilizes a model rocket propellant triggered by electric discharge for ignition purpose. The data acquisition system consists of Druck pressure transducers for static pressure, a PCB accelerometer for dynamic pressure, and a load cell by CAS for thrust and K-type thermocouples. The DAQ board and LabVIEW program is also used for the data acquisition process. A baseline test was conducted with PMMA fuel and gaseous oxygen to verify the experimental setup and test procedure. Baseline test results are also compared with results in the references. Test results in Figure 2 demonstrate good agreement with previous studies [2].

Swirl flow induced by the injector is known to increase the regression rate by increasing the contact time between the oxidizer and solid fuel. It is, however, generally known that the effect of swirl flow is only limited near the inlet part of the fuel port because swirl strength diminishes by the viscous interaction with the solid fuel surface as it flows downstream. A typical example of combustion with swirl flow in hybrid fuel can be found in reference [3]. So it is natural to seek a method not only to minimize the disadvantage of the swirl injector but to overcome the negative effects by using other options.

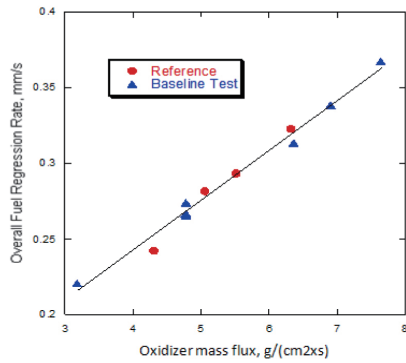


Fig. 2. Comparison of measured regression rate with reference one



Fig. 3. Helical grain configurations

In this respect, this study concentrates on the improvements of the swirl effect by using the internal grain configuration. Four different pitches are adopted in the experiment. These include a pitch of 3, 6, 12, and 18 as shown in Figure 3. Here, pitch is defined as the distance (in mm) between troughs of the helical grain configuration. Also, it should be noted that a helical grain is only imposed over the after half of the fuel surface to examine the effect of port grain configuration on the combustion enhancement. In addition, the pitch depth was fixed for all tests to simplify the test variables. It is not surprising to find that the additional grain configuration can lower the charging efficiency because of the additional vacancy of fuel by the helical groove along the port.

All fuels with pitch have the similar order of charging volume of only 1 or 2 % less than baseline. However, the burning surface area (A_b) increases substantially by adopting the helical grain configuration ranging from 10% up to 50%. Thus, it is expected that the increase in surface area can nominally lead to the same percentage increase in volume burning rate (\dot{V}) if the regression rate remains unchanged as shown in the equation;

$$\Delta \dot{V} = \Delta A_b \cdot \dot{r}, \quad (1)$$

Test results, however, showed that a fuel with pitch 3 revealed at most the highest increase in volume burning rate

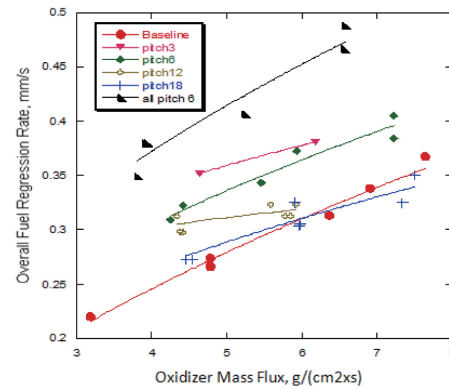


Fig. 4. Regression rates of several test cases with different pitch number from 3 to 18

(\dot{V}) of 5.075 cm³/s equivalent to a 35% increase compared with the baseline case, which is less than the 50% increase of surface area (A_b). This implies other mechanisms other than surface area are involved in controlling the volume burning rate with pitch configuration. One of the possible parameters can be the generation of turbulence caused by the helical configuration against the axial flow direction. The less pitch number is the more resistance to axial flow. Therefore, the stronger generation of turbulence in the flow may aggravate the volume burning rate.

Figure 4 summarizes test results for the regression rate of test cases with different pitch numbers from 3 to 18. Meanwhile, it is ambiguous to calculate the real burning surface area from measured port volume by using the port length of the fuel with pitch. Aside from the ambiguity, it is useful to calculate the regression rates of various fuel cases by using the simple relation of measured port volume, surface area and port length (L). As seen in the figure, pitch number can be one of the major variables affecting the regression rate. It is interesting to see that a fuel with pitch 3 shows the biggest increase in regression rate up to about 30% among test cases over the wide range of oxidizer flux from 3.2 g/(cm².s) to 7.6 g/(cm².s). Moreover, the test results show that fuel with a smaller pitch is effective in increasing the regression rate of the fuel.

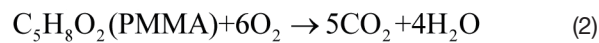
3. Combustion Visualization

Recent combustion tests with PMMA fuel by Lee et al. [5] found very interesting physical phenomena on the fuel surface during the combustion. Small scale dimples are randomly distributed on the fuel surface of PMMA. Also, some parts of the dimple are covered with dark unburned soot, which can be the manifestation of incomplete combustion. Figure 5 presents the overview of the dimples

found on the fuel surface and the magnified pictures of the surface near the end of PMMA fuel.

As in Figure 5, the size of spots near the injection plate is small and color is gray when compared to those found in the rest of fuel. Evans et al. [6] also reported a similar transition of surface patterns from smooth to rough in the combustion of HTPB/N₂O. The size of the rough surface on the fuel seems much bigger than those observed in the tests with PMMA. However, they did not claim the incomplete combustion on the rough surface because the HTPB color is dark black itself.

The combustion condition was checked by the use of stoichiometric chemistry to see if the combustion was occurred in the oxidizer rich condition. The stoichiometric reaction of PMMA with oxygen can be written as;



Furthermore, the simple calculation shows that the stoichiometric O/F ratio is 1.92, which is a much smaller value of the actual O/F ratio of 4.31. Thus, the combustion was occurred in the oxidizer rich condition. Notwithstanding this fact, dark spots with incomplete combustion are observed in the fuel surface, and this needs to be physically explained. The visualization of combustion was done with the aid of an opaque acryl plate and intensity reduction filter (ND8) used to control the total amount of light intensity to the digital camera. Tests were done for 10 seconds with an oxidizer mass flow rate of 20g/sec.

Fig. 6 shows the sequential progress of the combustion process with equal time intervals. PMMA was used as a fuel in a cylindrical shape. During the early stage of combustion (i.e. up to 3 seconds), streaky patterns reminiscent of typical turbulent structures are displayed. They are much more elongated in the streamwise direction. Later, however, isolated circular patterns appear and grow as the combustion progresses. The stage after the initiation of the combustion process is characterized by the increasing regression rate at the wall. As the regression process or wall blowing increases, this injected momentum starts to interact with the main flow.

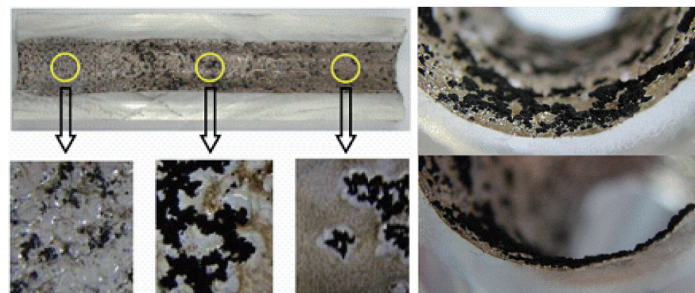


Fig. 5. Dimples on PMMA fuel surface and magnified view near the fuel en

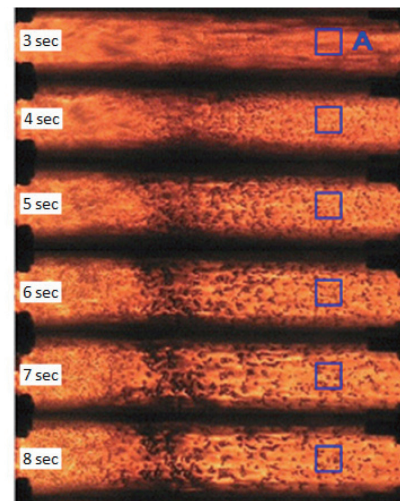


Fig. 6. Transition of surface morphology in PMMA combustion

Thus, the change of the observed pattern can be attributed to the disturbance incurred by the injection.

However, this pattern becomes somehow perturbed at 4 sec. and very tiny dark spots begin to form in the after half of the fuel surface. It should be noted that the concentrated distribution of dark spots in the middle of fuel is attributed to the sudden expansion of oxidizer flow from the pressure of 400 to 300 psi in the combustion chamber. Also, dark spots may grow into a bigger size during combustion or be swept away by the strong surface flow. It is very interesting to find that dark spots are barely observed at the head end whereas many spots are found at the after half of grain. Evans et al. [6] reported the similar results on the surface roughness in their experiments with HTPB/N₂O.

The difference in surface roughness between the front half and the after half may provide a clue of what the basic mechanism of the formation of dimples and dark spots is. A close examination on the fuel surface reveals that the formation of dark spots and dimples is related with the interaction of oxidizer flow with fuel flux. The next section will focus on the numerical analysis with LES to investigate the formation of dark spots and dimples.

4. Numerical Methodology

The most popular LES model is, perhaps, the dynamic Smagorinsky model (DSM). This model has been successfully applied to a various class of flows for the past 15 years. Even with the proven validity, its excessive dissipative nature causes a series of further modification of the model. One of such successful efforts is the so-called dynamic mixed model (DMM). This model, which has also been tested for a variety of flows, is known to have a better performance than its predecessor, DSM. Details on the methodology of DMM and its straightforward extension to the calculation of passive scalar will be found in Na. [5].

4.1 Governing equation for LES

Considering the fact that the flow velocity inside the hybrid motor remains relatively low compared to the sonic velocity in the accompanying experiment, the flow is assumed to be incompressible. Thus, the filtered transport equation for the passive scalar in addition to continuity and momentum equations are described as follow:

Governing equations are integrated in time using a semi-implicit procedure in Na. [5]. The convective term is treated by the 3rd order Runge-Kutta method and the viscous term is integrated by the 2nd order Crank-Nicolson scheme. All the spatial derivatives were conducted by the 2nd order central difference scheme except for the convective term of Eq. (3). Noting the fact that the central difference scheme for the convective term of the passive scalar equation suffers from numerical instability, this problem was effectively suppressed by the use of the popular QUICK scheme [6].

4.2 Computational Domain

The numerical domain is shown in Fig. 7. As was explained earlier, the model rocket motor was idealized by the simple

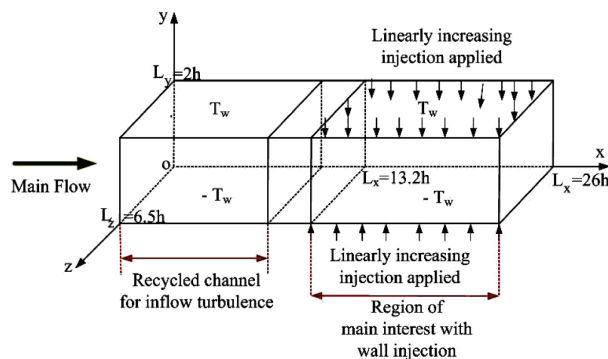


Fig. 7. Schematic of numerical domain

channel and the regression process is approximated by the injection of the fluid at the wall. Since the main scope of the present work is to examine the interaction of main and injected flows, which basically occur in the near-wall boundary layer, neglecting the curvature effect is not believed to deteriorate the validity of the present numerical result significantly.

In order to supply the physically realistic turbulence to the region of interest with wall injection, the flow is continuously recycled in the channel placed in front of the domain so that it allows the spatial room for developing realistic turbulence. It turns out that this device of flow configuration generates physically acceptable coherent structures making the present analysis very realistic from the point of flow dynamics.

Reynolds number based on inlet bulk velocity and the half channel height was set to 22,500, which is very close to that of the physical experiment and the Prandtl number was set to 1. A series of computations was conducted with different resolutions before we settled on the $513 \times 193 \times 513$ grid system (approximately 51 million grids). All the results shown here are based on this grid system.

4.3 Boundary condition

The no-slip boundary condition was assumed along the wall except in the second half of the channel where the injection is applied. The magnitude of the injected vertical velocity is varying linearly from 0% to 3% as was seen in the experiment. Constant temperatures were maintained along the walls with the lower wall at higher temperature. Since the temperature was assumed to be a passive scalar, having a higher temperature at the lower wall does not cause the density change. The periodic boundary condition was imposed in the spanwise direction and the convective boundary condition was specified at the exit in order to allow turbulence structures to leave the domain with minimal distortion.

5. Results

The contours of instantaneous streamwise velocity in the plane close to the wall (Fig. 8a) clearly show that the structural feature has been altered by the application of wall injection, which is, again, reminiscent of patterns of the isolated roughness found in the experiment (Fig. 6). This abrupt change of flow characteristics is accompanied by the rapid movement of coherent structures away from the wall. Using a method of vortex identification (eigenvalues of velocity gradient tensor), visualization of coherent structures

was made. A close examination of the iso-contours of coherent structures displayed in Fig. 5 reveals that the streaky structures generated upstream of wall injection (they tend to be aligned more or less in the main flow direction) are displaced away from the wall, leaving more isolated circular contours on the surface as a footprint. In addition to this displacement, the shear layer resulting from the interaction of main flow with the wall injection contributes to the abundant supply of coherent structures also seen in Fig. 8b.

Fig. 9 shows how the hydrodynamic and thermal boundary layers react to the wall injection. Flow experiences strongly accelerate due to the addition of mass through the wall and this results in strong inhomogeneity in the streamwise direction in the region of $x/h > 13.2$. Also, farther displacement of the thermal boundary layer away from the wall is evident in this figure. Since the temperature field was assumed as a passive scalar, this indicates that diffusions of momentum and passive scalar are occurring at different rates. Mean streamwise velocity and temperature profiles at several representative streamwise locations (Fig. 10) also imply that the friction temperature, which is relevant to the ratio of the velocity gradient and temperature gradient at the wall, becomes smaller in the region of wall injection. This sudden decrease of temperature gradient at the wall will eventually suppress the conduction heat transfer to the surface, resulting in the suppression of regression rate.

One of the main interests is the behavior of turbulence activity away from the wall. Fig. 11 illustrates the turbulent stress and heat flux in the normal wall direction at several locations. Due to the interaction of main oxidizer flow with the wall blowing, a very strong shear layer develops away from the wall. In this shear layer, coherent structures

multiply very rapidly as shown in Fig. 9 and cause a sudden increase of turbulent heat flux in the vertical direction as well as Reynolds shear stress. It is noted that the location of maximum heat flux is displaced further away from the wall than that of Reynolds shear stress. This behavior is consistent with the findings shown in both the instantaneous and statistical results given in Figs. 10 and 11.

Finally, the time-scale of the flow in the vicinity of the wall was pursued by inspecting the frequency spectra and auto correlation of streamwise velocity (Fig. 12). Note that, in the presence of wall blowing, very large negative excursion develops in the auto correlation. For reference, it should be noted that the location of $x/h=8.1$ corresponds to the simple change without wall injection. It is obvious that this unexpected feature reflects the complicated change regarding the structural feature of coherent structures. If Taylor's hypothesis is used here, the behavior in the time direction can be converted into that in the streamwise direction. The presence of a large negative correlation would mean that near-wall streaky structures are not as long as in upstream but they break down into several pieces due to the action of injection. This behavior is consistent with the appearance of isolated circular patterns in Fig. 8a. Since the vertical structures are too crowded in Fig. 9, it is not easy to measure the change of size of those structures but a more careful investigation is being conducted.

The frequency spectra also display the presence of a very distinctive peak near the non-dimensional value of frequency around 8 after the application of wall injection. This characteristic Strouhal number is much greater than that of typical vortex shedding flow configuration such as in the backward facing step [7,8]. Unfortunately, we are unable to find the origin for this behavior at the moment. A complete

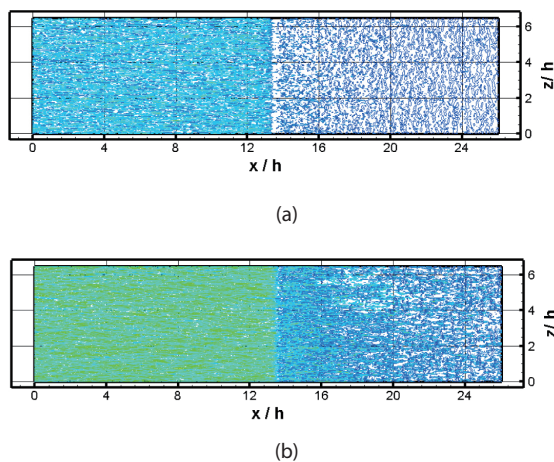


Fig. 8. Instantaneous snapshots of streamwise velocity at two different (x-z) planes

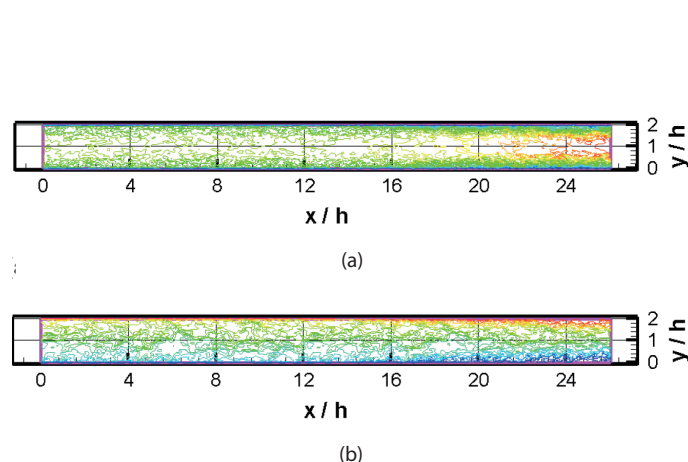


Fig. 9. Snapshots of instantaneous streamwise velocity and temperature at mid (x-y) plane

explanation will require more flow field information and this constitutes our future study.

6. Summary and Conclusion

The present paper was mainly intended to assess the role of helical grain configuration in the regression rate inside the hybrid rocket motor. In order to improve the regression rate, a combination of swirl (which is an active method) and helical grain (which is a passive method) was adopted. A series of experimental results suggest that the amount of increase in

the regression rate was found to depend on the pitches and the inflow condition. The followings are the summary:

Enhancement of regression rate can be achieved by combining both the helical grain configurations and swirl injector.

The measurement results showed that a better regression can be achieved in the case of pitch 6 rate than in the case of pitch 100 if no swirl is imposed at the inlet.

The regression rate in the case of pitch 100 was increased up to 250% compared to the baseline when swirl flow is imposed. This rate of increase was higher compared with the case of pitch 6 (240%).

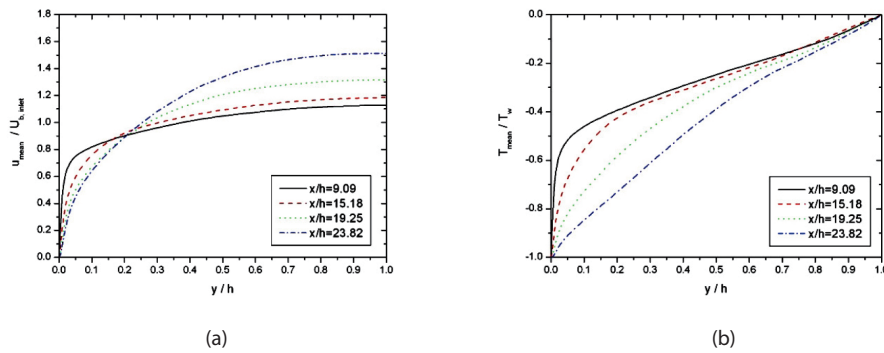


Fig. 10. Mean profiles at several location

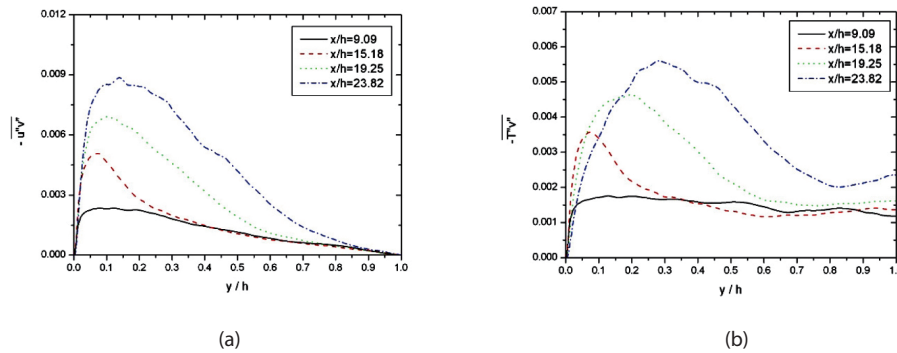


Fig. 11. Turbulent transport statistics at several location

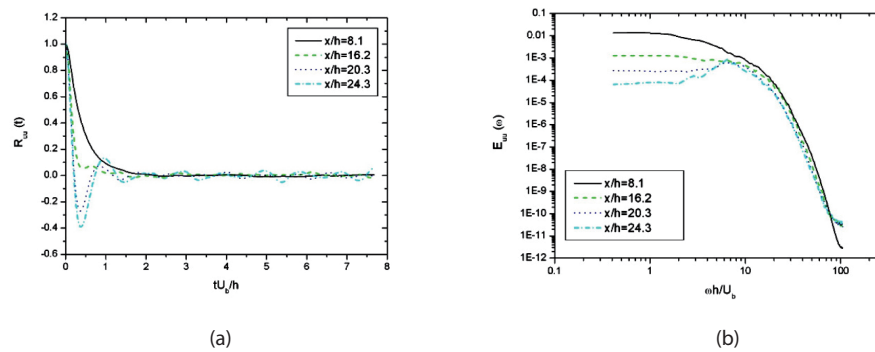


Fig. 12. Time characteristics of streamwise velocity in the vicinity of wall

Even though the present work suggests that the presence of the swirl component of velocity at the inlet of the rocket motor influences the subsequent flow evolution in terms of regression rate, any attempt of finding an optimum strength of swirl was not attempted. Also, the RANS type of numerical approach has its inherent limit in understanding the interaction between turbulent structures and the frequency of the pitch.

The large eddy simulation was also performed in an idealized model rocket motor with an objective of understanding the origin of isolated surface roughness patterns seen in several recent experiments. In particular, emphasis was put on the evolution of near-wall turbulent structures in the presence of wall injection. The flow is characterized by the non-negligible streamwise inhomogeneity due to the disturbance generated by injected flows at the wall. Several turbulent statistics and correlations indicate that the wall injection drastically changes the characteristics of the near-wall turbulence. Contours of instantaneous streamwise velocity in the plane close to the wall clearly show that the structural feature has been significantly altered by the application of wall injection, which is reminiscent of the isolated roughness patterns found in several experiments. This abrupt change of flow characteristics is accompanied by the rapid movement of coherent structures away from the wall. Close examination of the iso-contours of coherent structures reveal that the streaky structures generated upstream of wall injection are displaced away from the wall, leaving more isolated circular contours on the fuel surface. Thus, the sequential change of patterns observed in the experiment is believed to be strongly related to the change in kinematic configuration of near-wall structures.

Acknowledgments

This work was supported by 2011 research grants of

National Research Foundation (2011-0027980) in Korea. Author greatly appreciates the research support.

References

- [1] Humble, R. W., Henry, G. N., and Larson, W. J., *Space Propulsion Analysis and Design*, McGraw-Hill, Inc, New York, 1995.
- [2] Sutton, G.P. and Biblarz, O., *Rocket Propulsion Elements*, John Wiley & Sons, New York, 2001.
- [3] Yuasa, S., Yamamoto, K., Hachiya, H., Kitagawa, K., and Owada, Y., "Development of a Small Sounding Hybrid Rocket with a Swirling-Oxidizer-Type Engine", AIAA 2001-3537, *37th AIAA/ASME/SAE/ASEE, Joint Propulsion Conference & Exhibit*, Salt Lake City, Utah, 2001.
- [4] Shin, K. H., Lee, C., Chang, S. Y., and Koo, J. Y., "The Enhancement of Regression rate of hybrid Rocket Fuel by Various Method", AIAA 2005-0359, *41st AIAA/ASME/SAE/ASEE Joint Propulsion Conference and Exhibit*, Tucson, Arizona, 2005.
- [5] Lee, C. and Na, Y., "Large Eddy Simulation of Flow Development in Chamber with Surface Mass Injection", *Journal of Propulsion and Power*, Vol. 25, No. 1, 2009, pp. 51-59.
- [6] Evans, B., Favorito, N. A., and Kuo, K. K., "Oxidizer-Type and Aluminum Particle Addition Effects on Solid Fuel Burning Behavior", AIAA 2006-4676, *42nd AIAA/ASME/SAE/ASEE Joint Propulsion Conference and Exhibit*, Sacramento, CA, 2006.
- [7] Na, Y. and Lee, C., "Frequency Response of Turbulent Flow to Momentum Forcing in a Channel with Wall Blowing", *Journal of Korean Society for Aeronautical and Space Sciences*, No. 1, 2010, pp. 64-72.
- [8] Na, Y. and Lee, C., "Intrinsic Flow Oscillation in Channel Flow with Wall Blowing", AIAA 2008-5019, *44th AIAA/ASME/SAE/ASEE, Joint Propulsion Conference & Exhibit*, Hartford, CT, 2008.